Publishing House
AKAPIT

COMPUTER METHODS IN MATERIALS SCIENCE

Informatyka w Technologii Materiałów

Vol. 15, 2015, No. 4

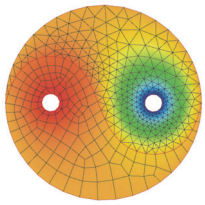

COMPUTATIONS OF RHEED INTENSITIES FOR GROWING SURFACES OF GaAs

ZBIGNIEW MITURA

AGH University of Science and Technology, Faculty of Metals Engineering and Industrial Computer Science, al. Mickiewicza 30, 30-059 Kraków, Poland
email: mitura@metal.agh.edu.pl

Abstract

A novel and practical algorithm for the determination of intensities in reflection high-energy electron diffraction (RHEED) for off-symmetry azimuths is presented. The usefulness of the algorithm is demonstrated for calculations of rocking curves for GaAs. Then the problem of RHEED oscillations that appear during regular growth of nanolayers is discussed. A calculated plot of the oscillation phase is compared with experimental data taken from the literature. Only the unreconstructed surface of GaAs is considered in this analysis, however, even for such a simplified case, the plot of the theoretical phase reproduces the experimental results reasonably well.

Key words: dynamical diffraction theory, nanolayers, RHEED intensity oscillations

1. INTRODUCTION

High-quality nanostructures can be realized in practice only if advanced methods to characterize the arrangement of atoms are used at different stages of sample preparation. A method of the great importance for the preparation of nanostructures under vacuum conditions is reflection high-energy electron diffraction (RHEED). However, it is interesting that this method is well developed only experimentally, as the theory of RHEED is still incomplete. Faithful theoretical approaches have been developed for perfectly flat surfaces (Ichimiya & Cohen, 2004; Peng et al., 2004). Precise computations that take into account multiple scattering effects are relatively fast for flat surfaces but become very time-consuming for disordered surfaces if large supercells are introduced. One of the possible ways to proceed is to try to develop faster methods of calculations with the help of iterative algorithms (Maksym et al., 1998; Mitura, 1999a; Maksym, 2001). Another possible alternative for further research is to carry out detailed analyses of data collected in particular situations and then return to general problems of partially ordered surfaces. An important example of such collected data are the results of measurements conducted for off-symmetry azimuths, i.e. when the azimuth of the incident beam direction is set a few degrees off the basic azimuth of the surface. Then simplifications in the theory can be introduced and respective computations can be carried out relatively easily. However, there are many important open questions even for this case. Thus, in this paper we focus on the off-symmetry case and deal with the problem of intensity oscillations which can be observed during regular growth of the material.

RHEED intensity oscillations can be observed if atoms deposited on the surface from a source do not merge in irregular islands of different heights, but form a new single monolayer of the material, and when such a layer is fully completed, the next layer of a similar type is formed on top and the procedure

ISSN 1641-8581

continues. When the intensity of the specularly reflected electron beam is recorded, periodic variations occur (for more details see: Herman & Sitter, 1996; Ichimiya & Cohen, 2004; Peng et al., 2004).

RHEED oscillations are observed if nanostructured layers are grown with the use of molecular beam epitaxy (for example, Fe layers can be prepared in such a way, see Olligs et al., 2002). The oscillations phenomenon may also appear if pulsed laser deposition is applied (for example, the preparation of TiN layers was reported for this case, Inumaru et al., 2000). At this point, it is not fully understood why these intensity oscillations occur. According to one of the proposed theoretical descriptions, RHEED oscillations occur because electrons are randomly scattered by step edges which appear at surface, periodically in time, during atom deposition (for example, Holmes et al., 1997). According to another approach, changes in the intensity result from changes in interference conditions for electron plane waves reflected from different atomic terraces (Pukite et al., 1988). In a third approach, it was proposed that RHEED oscillations may be caused by periodic changes in the averaged scattering potential at the surface (Peng & Whelan, 1990). Nevertheless, the approaches listed here require further verification and in this paper we examine the third approach in detail.

As stated above, no single theoretical description of RHEED oscillations has been widely accepted. Further investigations are required for achieving a better understanding of these oscillations through continued experimental measurements and data interpretations. Detailed calculations employing dynamical diffraction theory are needed if one wants to examine the approach in which oscillations occur because of changes in refraction conditions at the surface (Peng & Whelan, 1990). We proposed a new algorithm for these calculations which is very convenient for the development of respective computer codes.

Our paper is organized as follows: the algorithm for carrying out calculations for off-symmetry azimuths is shown in detail in section 2, in section 3 experimental data are briefly analyzed, and we present our conclusion in section 4.

2. A METHOD OF CALCULATIONS OF SPECULAR BEAM INTENSITIES

We describe here how to carry out dynamical calculations for the one-dimensional model of the potential that are suitable for analyzing data for the off-symmetry case. For completeness, we present a detailed formulation of the mathematical problem and a technique for determining the scattering potential. This is done although these issues were already discussed many times in the literature by different authors (see for example: Zhao et al.,1988; Ichimiya & Cohen, 2004; Peng et al., 2004; Mitura, 2013). However, different notations have been used and it seems helpful to display respective formulas in the form adopted by the current author. The novel and practical algorithm shown in this paper was developed by the present author and so far it was only briefly discussed in Mitura (2015). Here we give significantly more details.

2.1. Basic formulas

It is assumed that above the crystal surface the incident and reflected beams can be expressed with the help of the wavevectors $\mathbf{K}_i$ and $\mathbf{K}_f$, respectively, and the following relation is satisfied: $|\mathbf{K}_i|^2 = |\mathbf{K}_f|^2 = K^2$. Furthermore,

$$K^2 = \left(1 + \frac{|q_e|U}{2m_0c^2}\right)\frac{2m_0}{\hbar^2}|q_e|U. \qquad (1)$$

In equation (1), U is the absolute value of the accelerating voltage of the electron gun, q_e is the electron charge and m_0 is the electron rest mass. Additionally, $\hbar$ is Planck's constant and c is the speed of light in vacuum.

Before going further it useful to give detailed information on the values of the electron energy and the related quantity K^2. We assumed the energy of incident electrons to be 10 keV. Then, with the help of respective numerical data taken from Benenson et al. (2002), using equation (1), the value of 2650 Å^{-2} for K^2 was obtained (actually, we display here the value of K^2 with the four digit precision).

If we assume that the surface of the crystal is perpendicular to the z-axis, then above the crystal, i.e. for $z > z_T$, we can express the electron wavefield Ψ as follows

$$\Psi(\boldsymbol{r}) = \exp\{i[\mathbf{k}_{||}\cdot\boldsymbol{\rho} - k\,(z - z_T)]\} + r\exp\{i[\mathbf{k}_{||}\cdot\boldsymbol{\rho} + k\,(z - z_T)]\}, \qquad (2)$$

where $\mathbf{k}_{||}$ is the parallel component of the wavevectors $\mathbf{K}_i$ and $\mathbf{K}_f$, and $\boldsymbol{\rho}$ is the parallel component of the position vector $\mathbf{r}$. There are two terms in equation (2). The first term describes the incident beam (which is known) for which there exists the relation $k = |K|\sin\theta$, where θ is the glancing angle, i.e., the angle between the incident beam direction and the

surface. The second term in equation (2) describes the specularly reflected beam and its amplitude r needs to be determined. Finally, the intensity I of the reflected beam (the quantity that can be measured experimentally) is equal to $|r|^2$.

Within the crystal, the following Schrödinger equation is satisfied:

$$\nabla^2\Psi(\mathbf{r}) - v\,(z)\Psi(\mathbf{r}) + K^2\Psi(\mathbf{r}) = 0, \quad (3)$$

The potential $v(z)$ appearing in equation (3) can be found by summing the contributions $v_j(z)$ from all two-dimensional meshes of atoms. The meshes are parallel to the surface. For the j-th mesh placed at z_j, its contribution $v_j(z)$ can be expressed in the following form:

$$v_j(z) = -\Theta_j\left(1+\frac{|q_e|U}{m_0c^2}\right)\times(\gamma_{Re}+i\gamma_{Im})\frac{8\pi^{3/2}}{\Omega}\times \left\{\sum_l \frac{a_l^{(j)}}{\left(b_l^{(j)}+B^{(j)}\right)^{1/2}}\exp\left[-\frac{4\pi^2}{b_l^{(j)}+B^{(j)}}\left(z-z_j\right)^2\right]\right\}, \quad (4)$$

where $a_l^{(j)}$ and $b_l^{(j)}$ are coefficients of the analytical form of the elastic electron scattering factor for atoms of the j-th mesh, and $B^{(j)}$ is the temperature dependent Debye-Waller factor. For a crystal composed from identical atoms the superscript j for $a_l^{(j)}$, $b_l^{(j)}$ and $B^{(j)}$ could be dropped. However, generally different atoms need to be taken into account (actually this occurs for GaAs). The values of parameters for the elastic electron scattering factors are quite often set according to Doyle and Turner (1968), then four pairs of values of $a_l^{(j)}$ and $b_l^{(j)}$ would need to be used. However, we actually took the values from Peng et al. (2004) because it contains slightly more complete and accurate data. Five pairs of values of $a_l^{(j)}$ and $b_l^{(j)}$ for each mesh of atoms is required to be used in this case. As aforementioned, respective coefficients for Ga and As planes were taken from Peng et al. (2004). Further, the value of 2.0 Å^2 was set for all parameters $B^{(j)}$ appearing in equation (4). According to information given in Reid (1983) and in Schowalter et al. (2009), the number displayed above can be treated as a reasonable estimation of actual values of the Debye-Waller factors (both for Ga and As atoms) for the temperature of about 900 K, at which the material growth can be realized (Crook et al., 1989). Furthermore, Ω is the area of the two-dimensional mesh unit cell. For the case of the homoepitaxial growth of GaAs(001) layers, considered in the current paper, Ω is equal to $c_{latt}^2/2$, where c_{latt} is the lattice parameter and for which the value of 5.65 Å was assumed. Further, coming back again to equation (4), the coefficients γ_{Re} and γ_{Im} are additional parameters causing some corrections of the practical importance. The first parameter γ_{Re} is needed because there exists some deformation of electron wavefunctions for atoms constituting solids, i.e. their wavefunctions are not identical to those determined for isolated atoms. The second parameter γ_{Im} is needed because inelastic scattering events occur in the crystal. Thus, they are taken into account in a simplified manner by the introduction of the absorption of elastically scattered electrons. The modification of the real part of the potential and the introduction of its imaginary part can be realized in a number of different mathematical forms. The form applied by us is particularly suitable for growing surfaces. Actually, it is possible to determine the crystal potential with the corrections discussed above on the pure theoretical basis (see, for example, Radi, 1970). However, another approach is to use findings from interpretations of experimental data for identical or similar materials. The mean value of the potential real part can be determined experimentally reproducing positions of respective diffractions peaks and the mean value of the potential imaginary part can be found fitting widths of such peaks. In all calculations presented in this paper, we assumed that $\gamma_{Re} = 0.85$ and $\gamma_{Im} = 0.20$. We set these values with the help of findings from analyses of experimental data described in McCoy et al., (1992) and in Ohtake et al., (2002). Finally, Θ_j is the coverage of the j-th mesh, i.e., the ratio of the number of sites available to the number of the sites occupied, which is a very important parameter for cases when growing crystals are considered. It should also be mentioned that calculations employing the one-dimensional potential determined with the help of equation (4) can be used for the interpretation of experimental data for off-symmetry azimuths of the incident beam. For high-symmetry azimuths the use of the full three-dimensional scattering potential is more suitable (Ichimiya & Cohen, 2004; Mitura, 1999b).

Equations (1-4) define a mathematical problem; thus, we need to explain how to find the solution. One of the possibilities is to employ a numerical program used for solving general problems for the three-dimensional potential and to set input data properly. Such a route was used in some previous publications (for example in Mitura et al., 1998 and in Mitura, 1999b). If the general program developed within the two-dimensional Bloch wave theoretical framework is used for obtaining results for the case where the scattering potential varies only along the

z-axis, then calculations should be executed by considering the series of Bloch waves with only one term (respectively, this case is often named a one-beam approximation). However, actually such proceeding is not very efficient. Input data required for the general program contain some information which is not used at all for the case of one beam (for example positions of atoms in the $x-y$ plane). Furthermore, numerical calculations can be actually executed in a much simpler manner (for example, operations on matrices containing information on amplitudes of different scattered beams are not necessary). Thus, the case of the one-beam approximation can be treated separately and we herein describe a new algorithm developed specifically for such a case.

It is assumed that the crystal is infinite in $x-y$ planes. Further, two limiting planes, defined by $z=z_B$ and $z=z_T$ with the condition of $z_T>z_B$, are introduced and it is assumed that the crystal is contained between them. The distance between z_B and z_T is divided into W very thin slices having the same thickness h. The boundaries of the w-th slice are determined by z_{w-1} and z_w, where $z_w>z_{w-1}$. Additionally, it assumed that $z_0=z_B$ and $z_W=z_T$. For such a system of slices we determine a series of coefficients r_w, where w is an integer with values ranging from 0 to W. We begin with

$$r_0=0. \tag{5}$$

The other coefficients r_w are found computationally using the following formula:

$$r_w=\left\{r_{w-1}\left[1+h\left(ik+\frac{v_w}{2ik}\right)+\frac{h^2}{2}(-k^2+v_w)\right]+h\frac{v_w}{2ik}\right\}/\left\{1-h\left(ik+\frac{v_w}{2ik}\right)+\frac{h^2}{2}(-k^2+v_w)-r_{w-1}h\frac{v_w}{2ik}\right\}, \tag{6}$$

where v_w is the value of the potential in the middle point of the slice, i.e.,

$$v_w=v\left(\frac{z_{w-1}+z_w}{2}\right). \tag{7}$$

Finally, the amplitude r of the specularly reflected beam is given by

$$r=r_W. \tag{8}$$

A derivation of the algorithm defined by equations (5-8) is shown in section 2.3. Results obtained with the computer code based on this algorithm can be considered to be practically identical to those obtained using the general code described in detail in Mitura (1999b), for the case where the general code is adopted for calculations with the one-dimensional potential. The method given by equations (5-8) is much simpler than the method of Mitura (1999b). It is believed that the algorithm given in this paper can be used by experimental researchers for developing their own computer codes.

It should also be mentioned that specific algorithms for the one dimensional potential have already been shown in the past: in Peng and Whelan (1990) and in Ichimiya (1991). Our approach is different than the ones demonstrated by the authors of the above papers in the sense that we do not find the exact solution of differential equations within a slice, but rather employ Heun's method (Chapra & Canale, 2010) to obtain the numerical solution. Because of this fact, we do not need to use advanced mathematical functions of a complex variable. However, it seems that for our method, slices with smaller thicknesses may be required to achieve similar accuracy as in the case of the application of exact solutions within individual slices.

2.2. Testing results

To verify the method given by equations (5-8) we first carried out calculations of rocking curves for flat surfaces (see figure 1). Namely, the intensities of the specularly reflected electron beam were computed for different glancing angles of the incident beam. Calculations were carried out for two different values of the thickness of crystal slices. The number of slices per a unit cell was taken respectively to be 80 and 800. Slices with the thickness of 5.65/800 Å were found to be proper for carrying out precise computations. Namely, the further decrease of the slice thickness does not cause visible changes in results. However, for slices with the thickness of 5.65/80 Å, the calculated rocking curve is noticeably different than the curve determined for slices with the thickness of 5.65/800 Å (see figure 1). Thus the slice thickness of 5.65/80 Å seems to be too large for the use in calculations.

It is worth to recall here that GaAs is a compound with a zinc blende structure and its space group is F-43m. Further, the value of 5.65 Å is the size of the lattice parameter c_{latt} for GaAs. The (001) planes of the crystal contain alternately two-dimensional meshes of Ga and As atoms. We assumed in the current work that these planes are perpendicular to the z-axis. Additionally we assumed that at the surface there are only As atoms. Distances between atomic planes are equal to 5.65/4 Å, but

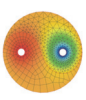

distances between planes of atoms of the same kind are equal to 5.65/2 Å. Calculations were carried out for the total length of $z_T - z_B$ equal to 110 × (5.65/4) Å. Within this distance, 101 atomic planes were taken into account.

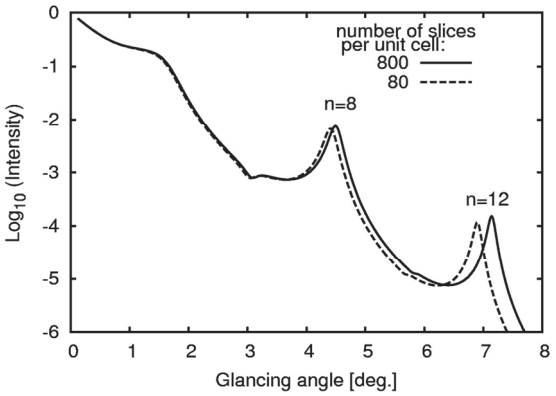

Fig. 1. *The intensity of the specularly reflected beam determined computationally for GaAs. Two different numbers of slices per a unit cell were used in calculations. The surface was assumed to be perfectly flat. Peaks are labeled according to the equation expressing the Bragg law with taking into account the refraction.*

The features of rocking curves computed with the help of equations (5-8) are generally difficult to explain because the intensity of the specularly reflected beam result from multiple scattering of electron waves. However, some concepts known from kinematical theory of X-ray diffraction may still turn out to be useful in the description of the rocking curves if they are applied with some modification. In particular, the Bragg law is known to be used for finding the conditions of the constructive interference of X-ray waves (Cullity, 1978; Bojarski et al., 2014). In fact, X-rays are usually very weakly scattered by atoms in a crystal. Such a condition is not satisfied for electrons, but the Bragg law can still be used even for this case if the effect of the refraction is properly taken into account. In order to get the improved formula we follow concepts given in Ichimiya (1992) and in Ichimiya and Cohen (2004). We start with a reminder of the Bragg law expressed in its basic form:

$$2d \sin\theta = n\,\lambda, \tag{9}$$

where d is the distance between atomic planes considered, λ is the wavelength and n is an integer. It is useful to rewrite equation (9) in the equivalent form:

$$|K| d \sin\theta = n\,\pi, \tag{10}$$

where $|K|$ is the magnitude of the incident beam wavevector. Now, if we want to take into account the effect of the refraction we need to modify equation (10). Accordingly, we can write the improved formula as follows:

$$\left|\tilde{K}\right| d \sin\tilde{\theta} = n\,\pi, \tag{11}$$

In equation (11), $|\tilde{K}|$ and $\tilde{\theta}$ mean the quantities corresponding to $|K|$ and θ, however, determined inside the crystal bulk. It is assumed here that the overall scattering properties of the crystal can described in a simplified manner with the help of $\tilde{v}_{Re}$, where $\tilde{v}_{Re}$ is the real part of the volume averaged scattering potential (to avoid theoretical complications, the imaginary part of the potential is ignored in the current considerations). There exists the following relation: $\tilde{K}^2 = K^2 - \tilde{v}_{Re}$. However, because the x-components and y-components of the corresponding wavevectors determined above the crystal and inside the crystal must be preserved, one can easily get another significant relation:

$$\tilde{K}^2 \sin^2\tilde{\theta} = K^2 \sin^2\theta - \tilde{v}_{Re}. \tag{12}$$

Combining equations (11) and (12) with simple mathematical manipulations, we get the following formula:

$$\sin^2\theta = \frac{n^2\pi^2 + \tilde{v}_{Re} d^2}{K^2 d^2}. \tag{13}$$

We should remind here that a similar formula (expressed in different notation) was shown in Ichimiya (1992). To use equation (13) in practice one needs to know the value of $\tilde{v}_{Re}$. This value can be determined on a theoretical basis. Starting from equation (4) and carrying out respective mathematical manipulations, one can obtain the following relation:

$$\tilde{v}_{Re} = -\left(1 + \frac{|q_e|U}{m_0 c^2}\right)\gamma_{Re}\frac{4\pi}{c_{latt}^3} \times \left(4\sum_l a_l^{(Ga)} + 4\sum_l a_l^{(As)}\right). \tag{14}$$

By using equation (14) one can find that the value of $\tilde{v}_{Re}$ is approximately equal to -3.483 Å^{-2}.

Actually, it is worth discussing what the practical consequences are for the inclusion of the term containing $\tilde{v}_{Re}$ in equation (13). Including this term causes shifts of Bragg peaks towards lower angles in relation to the predicted peak positions, when refraction is ignored. It is also worth adding that for electrons, at very small glancing angles, one should not expect the same total reflection that is observed in X-ray experiments. In more detail, the effect occurs for X-ray diffraction if the incident beam is nearly parallel to the surface. A similar effect can also be expected for positron diffraction (Ichimiya, 1992).

This is a consequence of the rule that refraction causes diffraction peaks to be shifted towards higher angles, for X-rays and positrons.

Altogether, using equations (13) and (14), we were able to determine approximate positions for Bragg peaks. We compared them with positions for peaks actually appearing in the rocking curve. The comparison was carried out for the rocking curves calculated with the division of the crystal into the slices with the thickness of 5.65/800 Å (the rocking curve is shown in figure 1 with the solid line). We set d= 5.65 Å and using equation (13) we carried out simple computations for different values of the integer n. Putting respectively n=4, 8 and 12 we found that Bragg peak should appear at θ=1.347º, 4.498º and 7.148º (the four digit precision was applied here). How were these values related to actual positions of peaks in the rocking curve? The second and the third numbers were in excellent agreement with the values of 4.49º and 7.14º found for the peaks in the rocking curve. The angular step for computing rocking curve intensities was equal to 0.01º, subsequently only three digits are shown for this case. However, upon analyzing the rocking curve, we were not able to clearly recognize the peak predicted for n=4. This peak appeared to be strongly deformed. It seems that this happened because at very small glancing angles, electrons penetrate mainly the topmost atomic planes and then the constructive interference of waves coming from the crystal bulk becomes less important. It should be also noted that peaks which one can predict with other values of n than aforementioned cannot be find analyzing the shape of the rocking curve. It seems that this can be explained on the basis of a detailed kinematical diffraction theory. Namely, the Bragg law given by equation (10) is derived assuming that only one family of atomic planes scatters waves. However, for GaAs, four such families need to be taken into account because there are four planes of atoms along the distance of 5.65 Å. Thus, even within kinematical approximation, the use of Bragg law must be combined with other rules. To obtain the detailed theoretical description for this situation one needs to take into account also the structure factor (Cullity, 1978) for the case of crystals with the structure of zinc blende (for which the space group is F-43m). This case is discussed in the book aforementioned. Respectively, for n with odd values peaks should not appear, for n=2, 6, 10 etc. only very small peaks are possible and for n=4, 8, 12 etc. strong peaks should appear. Such predictions are in agreement with the results of dynamical calculation shown in figure 1.

Finally, it is worth to discuss briefly the relation of the numerical algorithm given by equations (5-8) to possible RHEED measurements. It needs to be emphasized that only data collected for off-symmetry azimuths can be analyzed with its use. In fact, RHEED experiments are mostly conducted for symmetry azimuths and results of such experiments should be interpreted employing computer programs based on more general algorithms, i.e. developed for three-dimensional scattering potentials (Mitura, 1999b; Ichimiya & Cohen, 2004). For such cases precise modeling of atom arrangements at the surface seems to be crucial and this is why carrying respective theoretical analyses of experimental data is very difficult. In this paper we follow another approach. Namely, we are interested in the development of a theoretical description for RHEED data for off-symmetry azimuths. The virtues of such an approach were pointed out by Ichimiya and coworkers (Ichimiya, 1987; Kohmoto et al., 1989; Ichimiya, 1991). Respective measurements should be conducted after the selection of the azimuth of the incident electron beam to be few degrees off the symmetry direction of the crystal surface, where only one strong spot (caused by the specularly reflected beam) is visible at the screen (the intensities of other spots should be much weaker). Under such "one-beam conditions" the intensity of the specularly reflected beam is mostly sensitive to the positions of atoms along the axis perpendicular to the surface. Subsequently, theoretical analyses can be carried out in relatively simple way. Ichimiya and his coworkers conducted detailed research work of this kind for surfaces of Si. For GaAs, so far, similar work was not executed. However, we can admit that the algorithm developed by us is suitable for reproducing experimental one-beam rocking curves for static surfaces (i.e. for which structural arrangements of atoms do not change for relatively long time). This is because the results obtained with the use of equations (5-8) are expected to be practically identical with results obtained employing the algorithm shown in Ichimiya (1991). However, it is worth to note that before comparing results of calculations with experimental curves, in some situations, the introduction of an extra factor may turn out to be important. Namely, if during experiments the incident beam covers the entire sample, then results of calculations need to be earlier multiplied by $\sin\theta$ to take into account the specific geometry of experi-

ments (for discussion, see Ichimiya & Cohen, 2004). Further, for GaAs, detailed experimental data for the phase of oscillations were collected at one-beam conditions by Crook et al. (1989) and by Braun et al. (1998). We demonstrate in section 3.2 that the algorithm defined by equations (5-8) can be also used for analyses of such data.

2.3. Detailed theoretical considerations

In this section we describe how to obtain equation (6). The considerations presented here are not important for carrying out practical calculations. However, they constitute helpful information on the method used in the current work to determine the intensities of reflected electrons.

If we take into account the condition given by equation (2) we can write the solution $\Psi(\mathbf{r})$ of equation (3) in the following form

$$\Psi(\mathbf{r}) = \exp\left(i\boldsymbol{k}_{||}\cdot\boldsymbol{\rho}\right)\phi(z). \qquad (15)$$

If we rewrite equation (3) using the relation (15), after some manipulations, we obtain the following equation for $\phi(z)$

$$\frac{d^2\phi}{dz^2}(z) - v(z)\phi(z) + k^2\phi(z) = 0, \qquad (16)$$

where $k^2 = K^2 - |\mathbf{k}_{||}|^2$. We also have the relation $k = |K|\sin\theta$, θ is the glancing angle of the incident beam. If we next assume that the crystal is contained between two planes determined by $z = z_B$ and $z = z_T$, where $z_T > z_B$, we can determine the boundary conditions for $\phi(z)$. Namely, it follows from the basic description of the experimental conditions and equation (15) that above and below the crystal, $\phi(z)$ should have the following form

$$\phi(z) = \exp[-ik(z - z_T)] + r\exp[+ik(z - z_T)] \quad \text{for } z \geq z_T \qquad (17)$$

and

$$\phi(z) = t\exp[-ik(z - z_B)] \quad \text{for } z \leq z_B. \qquad (18)$$

Equations (16-18) define the problem that needs to be addressed, and the specular beam intensity I, which should be found, satisfies the relation $I = |r|^2$.

Let us define new variables $p^+(z)$ and $p^-(z)$:

$$\begin{cases}\frac{d\phi}{dz}(z) = ikp^+(z) - ikp^-(z)\\ \phi(z) = p^+(z) + p^-(z)\end{cases}. \qquad (19)$$

One can verify that solving the problem given by equation (16) can be replaced by solving the following set of differential equations (written with the help of matrix notation):

$$\begin{bmatrix}\frac{dp^+}{dz}(z)\\ \frac{dp^-}{dz}(z)\end{bmatrix} = \mathcal{A}(z)\begin{bmatrix}p^+(z)\\ p^-(z)\end{bmatrix}, \qquad (20)$$

where

$$\mathcal{A}(z) \equiv \begin{bmatrix}ik + v(z)/(2ik) & v(z)/(2ik)\\ -v(z)/(2ik) & -ik - v(z)/(2ik)\end{bmatrix}. \qquad (21)$$

Accordingly, the following boundary conditions should be satisfied:
for $z \geq z_T$:

$$\begin{cases}p^+(z) = r\exp[+ik(z - z_T)]\\ p^-(z) = \exp[-ik(z - z_T)]\end{cases}, \qquad (22)$$

and
for $z \geq z_B$:

$$\begin{cases}p^+(z) = 0\\ p^-(z) = \mathrm{t}\exp[-ik(z - z_B)]\end{cases}. \qquad (23)$$

The basic goal is to determine the value of r.

To determine r we can use Heun's method of solving differential equations (Chapra & Canale, 2010) after adding some mathematical operations. Let us first recall that Heun's method can be generally applied for solving the equations having the form $d\mathbf{y}/dz = \mathbf{f}(z, \mathbf{y})$, where x is an independent variable and $\mathbf{y}$ and $\mathbf{f}$ are vectors. If the solution $\mathbf{y}$ is known for some x then $\mathbf{y}(x + h)$ can be determined using the trapezoidal rule of the numerical integration and Euler's method. Namely, $\mathbf{y}(x + h) \simeq y(x) + (h/2)\left(\mathbf{f}(x, \mathbf{y}(x)) + \mathbf{f}(x + h,\ \mathbf{y}(x + h))\right)$ and additionally $\mathbf{f}(x + h,\ \mathbf{y}(x + h))$ is approximated by $\mathbf{f}(x + h,\ \mathbf{y}(x) + h\,\mathbf{f}(x, \mathbf{y}(x)))$. After the mathematical manipulation, we obtain the following relation

$$\begin{bmatrix}p^+(z + h)\\ p^-(z + h)\end{bmatrix} \simeq \mathcal{M}(z, h)\begin{bmatrix}p^+(z)\\ p^-(z)\end{bmatrix}, \qquad (24)$$

where

$$\mathcal{M}(z, h) = \mathcal{I} + \frac{h}{2}[\mathcal{A}(z + h) + \mathcal{A}(z)] + \frac{h^2}{2}\mathcal{A}(z + h)\mathcal{A}(z), \qquad (25)$$

In equation (25), $\mathcal{I}$ is the unity matrix.

If the crystal thickness is relatively thin (let us say, up to 10 Å then the system (20-23) can be rather easily solved stepping from the crystal bottom up to the crystal top assuming the initial conditions $p^+(z_B) = 0$ and $p^-(z_B) = 1$ at the crystal bottom.

Then at the crystal top we should obtain $p^+(z_T)$ and $p^-(z_B)$ satisfying relations $p^+(z_T) = r/t$ and $p^-(z_T) = 1/t$ (this a consequence of the linearity of the system). Finally, we can determine r from the relation $r = p^+(z_T)/p^-(z_T)$. However, generally, this is not the ideal approach for proceeding. For thick crystals (such situations are typical in practice), the coefficient t can be very small because of the assumed absorption of elastically scattered particles and/or multiple scattering effects. Thus, if we proceed as described, very large numerical values may appear at the crystal top, which may lead to the appearance of computational errors. It is more reasonable to divide the crystal into W slices and, at the top of each slice, and computationally determine r_w, where $w = 1, \ldots, W$. This process is realized in the following way. We use equation (24) assuming that at the bottom of each slice the initial conditions have the form

$$\begin{cases} p^+(z_{w-1}) = r_{w-1} \\ p^-(z_{w-1}) = 1 \end{cases}, \tag{26}$$

Additionally we approximate $\mathcal{A}(z+h)$ and $\mathcal{A}(z)$ by $\mathcal{A}(z+h/2)$. Then at the top of the w-th slice we have

$$\begin{cases} p^+(z_w) = r_{w-1}\left[1 + h\left(ik + \frac{v_w}{2ik}\right)\right] + \\ \quad r_{w-1}\left[\frac{h^2}{2}(-k^2 + v_w)\right] + h\frac{v_w}{2ik} \\ p^-(z_w) = 1 - h\left(ik + \frac{v_w}{2ik}\right) + \\ \quad \frac{h^2}{2}(-k^2 + v_w) - r_{w-1}h\frac{v_w}{2ik} \end{cases}, \tag{27}$$

where h is the slice thickness and v_w is the value of the potential at the slice midpoint, i.e.,

$$v_w = v\,(z_{w-1} + h/2). \tag{28}$$

Furthermore, r_w is determined by the relation $r_w = p^+(z_w)/p^-(z_w)$. Finally, equation (6) shown in section 2.1 is obtained from equation (27). Additionally, we assume that at the crystal bottom there exists only the transmitted wave, i.e. that $r_0 = 0$. Also we assume that r_w computed for the topmost slice is equal to r, which needs to be determined.

3. ANALYSIS OF INTENSITIES FROM GROWING SURFACES

3.1. Rocking curves for growing surfaces

As already discussed in section 2.2, rocking curves are sets of intensities determined for different glancing angles of the incident beam. If we assume that we are only interested in specular beam rocking curves we can say that such curves are similar to $\theta - 2\theta$ spectra that are known to researchers applying the X-ray technique who collect data using Bragg-Brentano geometry (for example, Castaño et al., 1997). In regards to RHEED, experimental rocking curves can be measured mainly for carefully prepared static surfaces. Then the direction of the incident electron beam can be slowly varied and respective intensities of the specularly reflected beam can be measured. However, if atoms of some material are deposited at the surface, then measurements of rocking curves become very difficult to conduct. It is much easier to observe changes in the RHEED pattern at the screen while keeping the direction of the incident beam fixed. If the growth of the material is regular, sometimes, oscillations of the specular beam intensity may occur (they will be discussed in detail in section 3.2). However, for carrying out theoretical analyses, rocking curves for growing surfaces are still important. Some features of the intensity oscillations for a fixed angle can be understood if the behavior of peaks of rocking curves is analyzed in detail, as discussed in Mitura et al. (1999).

We present here three rocking curves computed for different coverages of the topmost layer (see figure 2). It was assumed that the growing layer was composed from one Ga atomic layer and from one As atomic layer, with the total thickness equal to 5.65/2 Å. As atoms were assumed to be at the top of the crystal. The growing layer is effectively described with only one parameter: its coverage Θ. In fact, in this paper we ignored possible reconstructions at the surface, i.e. possible changes of the structural arrangement of atoms in relation to the arrangement of atoms at the crystal bulk (for respective information on the surface reconstructions for GaAs, see for example, Dabrawska-Szata, 2004; Ohtake, 2008). We also ignored possible increase of amplitudes of thermal vibrations near the surface (assuming that thermal displacements for Ga and As atoms are identical as mentioned in section 2). This is because we wanted to focus on the presentation of the main possibilities of the numerical algorithm given by equations (5-8). However, the use of more detailed models of the surface is important for detailed analyses (see Mitura et al., 1998; Mitura & Dudarev, 2015).

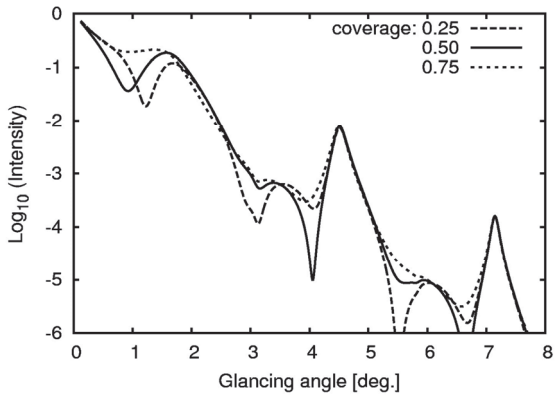

Fig. 2. Computed rocking curves for GaAs (001) for different coverages Θ of the growing layer.

We can observe large differences between the three curves shown in in figure 2. Generally the shapes of rocking curves for growing surface are not very simple for the explanation because of the superposition of many diffraction effects occurring in the crystal. However, it is particularly important that there are some angular shifts of respective peaks. Because of such shifts, large oscillating changes in the specular beam intensity appear if the intensity is recorded in time during the deposition of new layers of the material.

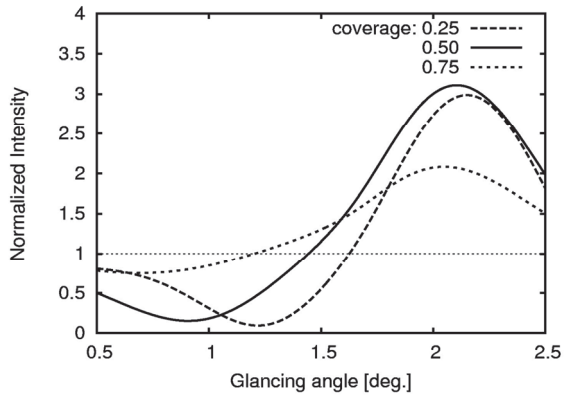

Fig. 3. Normalized rocking curves found computationally for GaAs (001) for different coverages Θ of the growing layer. Additional horizontal line is drawn for the value of 1 for easier comparisons of curves.

Large changes aforementioned can be recognized with the help of normalized rocking curves (see figure 3). Namely, the normalized intensity $J(\Theta)$ can be determined as follows: $J(\Theta) = I(\Theta)/I(0)$, where $I(\Theta)$ is the specular beam intensity for the coverage Θ and $I(0)$ is the specular beam intensity for the flat surface (i.e. for the growing layer coverage equal to 0). It should be added that we assume here that both $I(\Theta)$ and $I(0)$ refer to the same glancing angle. Taking a look at figure 3 one can recognize that for some values of the glancing angles the intensities of the specular beam for growing surfaces are much larger than corresponding intensities for the fat surface.

3.2. Intensity oscillations

Nowadays it is popular to monitor the preparation of nanostructures with the help of RHEED (for example, Sadowski et al., 2007). Moreover, if molecular beam epitaxy or pulsed laser deposition are used to prepare thin layers then regular oscillations of the intensity sometimes are observed. In detail, the intensity of the specularly reflected electrons can be recorded as a function of the time for a fixed direction of the incident electron beam. If the growth of the material follows the layer-by-layer growth mode then oscillating changes appear in the intensity recorded. The period of such changes corresponds to the deposition of a monolayer of the material (Herman & Sitter, 1996; Ichimiya & Cohen, 2004; Peng et al., 2004). Observations of RHEED oscillations are helpful in the preparation of highly ordered nanolayers. However, it is not quit clear why the oscillations appear. As mentioned in section 1 different explanations have been proposed. In this work we assume that the oscillations are a consequence of periodic changes in the laterally averaged scattering potential at the surface (i.e., we assume that they are caused by changes in refraction conditions).

We computed RHEED oscillations using the model described in section 2. In figure 4 three examples of runs of oscillations are shown. In fact in figure 4 runs of oscillations of different kind are displayed. One run is for oscillations with double minima. Two other runs is an example of a pair of oscillations having opposite phases. Concerning oscillations with double minima they are indeed very interesting. For the assumed growth of GaAs (001) such oscillations appear in computer simulations for glancing angles from the range of 0-0.8º. For the growth of some materials such oscillations can be sometimes observed experimentally (for more details, see Mitura, 1999b and Ichimiya & Cohen, 2004). However, in this paper we focus on the problem of the phase of oscillations.

It seems to be useful if parameters of experimental oscillations plotted as functions of the glancing angle are determined. Generally different parameters can be defined. It should possible to explain in detail such plots using the complete theory of RHEED oscillations. However, as mentioned earlier such theory still needs to be developed. From this point of view, it is important to point out that plots of the phase of oscillations as the functions of the

glancing angle seem to be especially suitable for testing possible theoretical approaches.

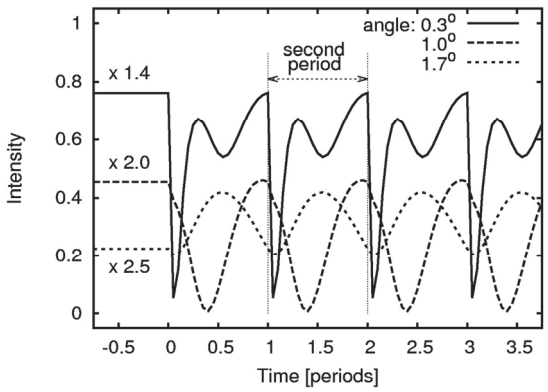

Fig. 4. *Three runs of RHEED oscillations determined computationally for different glancing angles θ (values of θ are given in the figure). Vertical lines are drawn to show the second period of oscillations. The exact times of the occurrence of oscillation minima in this period can be used to determine the phase of oscillations.*

The phase of the oscillations for a fixed glancing angle can be defined as the exact time of occurrence of the intensity minimum in the second period of oscillations (Zhang et al., 1987) divided by the time of lasting of one period of oscillations. Usually, the phase of experimental oscillations is not constant if the glancing angle of the incident beam is varied. However, according to the columnar approach (for example, Pukite et al., 1988) and to the step density approach (for example, Holmes et al., 1997), the minimum of the intensity should be observed if the coverage of the topmost layer is equal to 0.50. According to the approach in which the scattering potential of the growing layer is taken to be proportional to its coverage, the phase changes if diffraction conditions are varied (Peng & Whelan, 1990). A detailed verification is still needed for the above approach and actually its modification or extension may turn out to be necessary to get the fully quantitative description of RHEED oscillations.

Two plots of the phase of oscillations are shown in figure 5. Experimental results are taken from the literature (Crook et al., 1989). They are compared with theoretical results obtained using the algorithm given in section 2.1. The phase is denoted $t_{3/2}/T$ (such a special symbol introduced by Zhang et al., 1987 is common in the use by researches dealing with RHEED oscillations). In our work, to determine the theoretical plot, the reflected beam intensities were first calculated for twenty values of the coverage Θ of the growing layer. Then, for each glancing angle, the coverage Θ_{min} was computationally determined. Θ_{min} indicates the value of the coverage between 0 and 1, for which the intensity reaches the minimum in the period. Finally, $t_{3/2}/T = \Theta_{\min} + 1$. Values of $t_{3/2}/T$ determined in this manner satisfy the condition $1 \leq t_{3/2}/T < 2$.

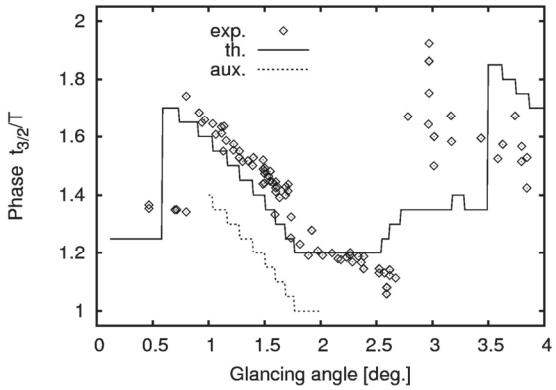

Fig. 5. *A comparison of the experimental oscillation phases with the results of computations. The experimental data taken from the literature (Crook et al., 1989) are shown with diamonds. The solid line is for the results of the calculations assuming that the regular homoepitaxy starts with some time delay (equal to 0.20 of the period). The auxiliary, dash line shown in the angular region of 1°-2° is for the results of the calculations where it is assumed that regular growth starts without any time delay.*

In fact we found it beneficial to add some small number to all values of the phase found theoretically. In other words it can be said that we found helpful to introduce the small vertical shift of the theoretical plot. The theoretical plot shown in figure 5 was obtained after respective adding the constant equal to 0.2. How do we explain the need to apply this small shift? It seems that in experiment there are some disturbances of vacuum conditions at the sample surface just after starting the growth of the material and this needs to be taken into account also in calculations. In a sense we assumed that a regular homoepitaxy started with the time delay equal to 0.2 of the period.

One can observe a reasonably good agreement between the experimental and theoretical plots of the phase (see figure 5). At higher glancing angles there exist a number of discrepancies between the plots shown. However, the discrepancies become smaller if specific arrangements of atoms at the surface are taken into account, i.e. if details of the surface reconstruction are included in analysis (as discussed in Mitura et al., 1998; Mitura & Dudarev, 2015). However, one can learn from the plots displayed in figure 5 that even ignoring details of the reconstruction one should be able to carry out basic interpretations of experimental data for off-symmetry azimuths if he/she applies the theoretical approach in which

changes in refraction conditions are properly described.

It is worth mentioning that the direct determination of the oscillations phase in some situations can be replaced by the Fourier method of analyzing oscillations runs. The direct method is easier in practice, however, the Fourier method allows one to remove small disturbances in the intensities (Mitura et al., 1998; Mitura & Dudarev, 2015).

4. CONCLUSIONS

It was shown in this work that periodic changes in the refraction conditions constitute an important cause for the appearance of RHEED oscillations. However, to get better understanding of the phenomenon of oscillations, more experimental data should be collected and then analyzed in detail. We think that the algorithm for dynamical calculations described in this paper may turn out to be effective in carrying out research work of this kind. To make the presentation of the numerical algorithm more comprehensive, we assumed that the surface of GaAs was unreconstructed, i.e. the arrangement of atoms at the surface was taken to be similar like in the crystal bulk. However, it should be emphasized that for GaAs(001) the effects caused by actual structural ordering of atoms at the topmost layers are important, as discussed in Mitura and Dudarev (2015). In general, further investigations are required to construct the fully quantitative description of electron diffraction for growing surfaces.

ACKNOWLEDGMENTS

This research was supported by AGH Project No. 11.11.110.291.

REFERENCES

Benenson, W., Harris, J.W., Stocker H., Lutz, H., eds., 2002, *Handbook of Physics*, Springer-Verlag, New York.

Bojarski, Z., Gigla, M., Stróż, K., Surowiec, M., 2014, *Krystalografia*, third edition, PWN, Warsaw (in Polish).

Braun, W., Däweritz, L., Ploog, K.H., 1998, New model for reflection high-energy electron diffraction intensity oscillations, *J. Vac. Sci. Technol. B*, 16, 2404-2412.

Castaño, F.J., Stobiecki, T., Gibbs, M.R.J., Czapkiewicz, M., Kopcewicz, M., Gacem, V., Speakman, J., Cowlam, N., Blythe, H.J., 1997, Structural and magnetic properties of amorphous Fe/Zr multilayers, *J. Phys.: Condens. Matter*, 9, 10603-10614.

Chapra, S. C., Canale, R.P., 2010, *Numerical Methods for Engineers*, sixth edition, McGraw–Hill, New York.

Crook, G. E., Eyink, K. G., Campbell, A. C., Hinson, D. R., Streetman, B. G. (1989), Effects of Kikuchi scattering on reflection high-energy electron diffraction intensities during molecular-beam epitaxy GaAs growth, *J. Vac. Sci. Technol. A*, 7, 2549-2553.

Cullity, B.D., 1978, *Elements of X-Ray Diffraction*, second edition, Addison-Wesley, Reading.

Dabrowska-Szata, M., 2004, RHEED study of reconstructed GaAs(001) surfaces, eds. Morawiec, H., Stróż, D., *Applied Crystallography, Proceedings of XIX Conference*, World Scientific, Singapore, 316-319.

Doyle, P.A., Turner, P.S., 1968, Relativistic Hartree-Fock X-ray and electron scattering factors, *Acta Cryst. A*, 24, 390-397.

Herman, M.A., Sitter, H., 1996, *Molecular Beam Epitaxy: Fundamentals and Current Status*, second edition, Springer-Verlag, Berlin.

Holmes, D.M., Sudijono, J.L., McConville, C.F., Jones, T.S., Joyce, B.A., 1997, Direct evidence for the step density model in the initial stages of the layer-by-layer homoepitaxial growth of GaAs(111)A, *Surface Sci.*, 370, L173-L178.

Ichimiya, A., 1987, RHEED intensity analysis of Si(111)7x7 at one-beam condition, *Surface Sci.*, 192, L893-L898.

Ichimiya, A., 1991, One-beam RHEED for surface structure analysis, eds., Tong, S.Y., Van Hove, M.A., Takayanagi, K., Xie, X.D., *The Structures of Surfaces III*, Springer–Verlag, Berlin, 162-167.

Ichimiya, A., 1992, Reflection high-energy positron diffraction (RHEPD), *Solid State Phenomena*, 28-29, 143-148.

Ichimiya, A., Cohen, P.I., 2004, *Reflection High Energy Electron Diffraction*, Cambridge University Press, Cambridge.

Inumaru, K., Ohara, T., Yamanaka, S., 2000, Pulsed laser deposition of epitaxial titanium nitride on MgO(001) monitored by RHEED oscillation, *Appl. Surface Sci.*, 158, 375-377.

Kohmoto, S., Mizuno, S., Ichimiya, A., 1989, RHEED intensity analysis of Li/Si(111) structures, *Appl. Surface Sci.*, 41-42, 107-111.

Maksym, P.A., 2001, Investigation of iterative RHEED calculations, *Surface Sci.*, 493, 1-14.

Maksym, P.A., Korte, U., McCoy, J M., Gotsis, H.J., 1998, Calculation of RHEED intensities for imperfect surfaces, *Surf. Rev. Lett.*, 5, 873-880.

McCoy, J.M., Korte, U., Maksym, P.A., Meyer-Ehmsen, G., 1992, Analysis of RHEED data from the GaAs(001)2x4 surface, *Surface Sci.*, 261, 29-47.

Mitura, Z., 1999a, Iterative method of calculating reflection-high-energy-electron-diffraction intensities, *Phys. Rev. B*, 59, 4642-4645.

Mitura, Z., 1999b, RHEED from epitaxially grown thin films, *Surf. Rev. and Lett.*, 6, 497-516.

Mitura, Z. Dudarev, S.L., Whelan, M.J., 1998, Phase of RHEED oscillations, *Phys. Rev. B*, 57, 6309-6312.

Mitura, Z., Dudarev, S.L., Whelan, M.J., 1999, Interpretation of reflection high-energy electron diffraction oscillation phase, *J. Cryst. Growth*, 198/199, 905-910.

Mitura, Z., 2013, Computer studies on reflection high-energy electron diffraction from the growing surface of Ge(001), *J. Appl. Cryst.*, 46, 1024-1030.

Mitura, Z., 2015, Theoretical analysis of reflection high-energy electron diffraction (RHEED) and reflection high-energy positron diffraction (RHEPD) intensity oscillations expected for the perfect layer-by-layer growth, *Acta Cryst. A*, 71, 513-518.

Mitura, Z., Dudarev, S.L., 2015, Algorithms for determining the phase of RHEED oscillations, *J. Appl. Cryst.*, 48, 1927-1934.

Ohtake, A., 2008, Surface reconstructions on GaAs(001), *Surface Sci. Rep.*, 63, 295-327.

Ohtake, A., Ozeki, M., Yasuda, T., Hanada T., 2002, Atomic structure of the GaAs(001)-(2x4) surface under As flux, *Phys. Rev. B*, 65, 165315.

Olligs, D., Bürgler, D.E., Wang, Y.G., Kentzinger, E., Rücker, U., Schreiber, R., Brückel, Th., Grünberg, P., 2002, Roughness-induced enhancement of giant magnetoresistance in epitaxial Fe/Cr/Fe(001) trilayers, *Europhys. Lett.*, 59, 458-464 .

Peng, L.-M., Whelan, M.J., 1990, Dynamical RHEED from MBE growing surfaces, *Surface Sci.*, 238, L446-L452.

Peng, L.-M. , Dudarev, S.L., Whelan, M.J., 2004, *High-Energy Electron Diffraction and Microscopy*, Oxford University Press, Oxford.

Pukite, P.R., Cohen, P.I., Batra, S., 1988, The contribution of atomic steps to reflection high energy electron diffraction from semiconductor surfaces, eds, Larsen, P.K., Dobson, P.J., *Reflection High Energy Electron Diffraction and Reflection Electron Imaging of Surfaces*, Plenum Press, New York, 427-447.

Radi, G., 1970, Complex lattice potentials in electron diffraction calculated for a number of crystals, *Acta Cryst. A*, 26, 41-56.

Reid, J.S., 1983, Debye-Waller factors of zinc-blende-structure materials - a lattice dynamical comparison, *Acta Cryst. A*, 39, 1-13.

Sadowski, J., Dłużewski, P., Kret, S., Janik, E., Łusakowska, E., Kanski, J., Presz, A., Terki, F., Charar, S., Tang, D., 2007, GaAs:Mn nanowires grown by molecular beam epitaxy of (Ga,Mn)As at MnAs segregation conditions, *Nano Letters*, 7, 2724-2728.

Schowalter, M., Rosenauer, A., Titantah, J.T., Lamoen, D., 2009, Computation and parametrization of the temperature dependence of Debye–Waller factors for group IV, III–V and II–VI semiconductors, *Acta Cryst. A*, 65, 5-17.

Zhao, T.C., Poon, H.C., Tong, S.Y., 1988, Invariant-embedding R-matrix scheme for reflection high-energy electron diffraction, *Phys. Rev. B*, 38, 1172-1182.

Zhang, J., Neave, J.H., Dobson, P.J., Joyce, B.A., 1987, Effects of diffraction conditions and processes on RHEED intensity oscillations during the MBE growth of GaAs, *Appl. Phys. A*, 42, 317-326.

OBLICZENIA NATĘŻEŃ WIĄZKI ELEKTRONÓW ODBITYCH ZWIERCIADLANIE OD WZRASTAJĄCYCH POWIERZCHNI, DLA ARSENKU GALU

Streszczenie

Zaprezentowano nowy, praktyczny algorytm komputerowy do wyznaczania natężeń wiązki zwierciadlanej dla dyfrakcji odbiciowej elektronów wysokoenergetycznych (zakłada się, że padająca wiązka elektronów nie pokrywa się z kierunkami osi symetrii powierzchni kryształu). Użyteczność algorytmu zademonstrowano w obliczeniach krzywych odbicia dla arsenku galu. Następnie omówiono zagadnienie charakterystycznych oscylacji natężenia wiązki odbitej zwierciadlanie, które pojawiają się, gdy wzrost warstw nanostrukturalnych odbywa się w sposób bardzo regularny. W szczególności przeprowadzono porównanie literaturowego wykresu fazy oscylacji uzyskanego na podstawie pomiarów z wykresem sporządzonym na podstawie obliczeń. Uzyskano dobrą zgodność wyników eksperymentalnych i teoretycznych, chociaż w pracy rozważano tylko najprostszy model powierzchni kryształu arsenku galu.

Received: August 8, 2015
Received in a revised form: November 24, 2015
Accepted: December 15, 2015